

¹ Thresholdmann: A Web tool for interactively creating adaptive thresholds to segment MRI data.

³ **Katja Heuer**  ¹, **Nicolas Traut**  ¹, and **Roberto Toro**  ¹

⁴ **1** Institut Pasteur, Université Paris Cité, Unité de Neuroanatomie Appliquée et Théorique, F-75015 Paris,
⁵ France

DOI: [10.xxxxxx/draft](https://doi.org/10.xxxxxx/draft)

Software

- [Review](#) 
- [Repository](#) 
- [Archive](#) 

Editor: 

Submitted: 11 December 2023

Published: unpublished

License

Authors of papers retain copyright and release the work under a Creative Commons Attribution 4.0 International License ([CC BY 4.0](https://creativecommons.org/licenses/by/4.0/))

⁶ Summary

⁷ Brain extraction and segmentation are the first step for most neuroimaging analyses. Automatic
⁸ methods work well in adult human brains, but produce unreliable results in non-human data,
⁹ due to muscle tissue, skull, and luminosity gradients. Thresholdmann (<https://neuroanatomy.github.io/thresholdmann>) is an open source Web tool for the interactive application of space-
¹⁰ varying thresholds to Nifti volumes. No download or installation are required and all processing
¹¹ is done on the user's computer. Nifti volumes are dragged and dropped onto the Web app
¹² and become available for visual exploration in a stereotaxic viewer. A space-varying threshold
¹³ is then created by setting control points, each with their own local threshold. Each point
¹⁴ can be repositioned or removed, and each local threshold can be adjusted in real time using
¹⁵ sliders or entering their values numerically. The threshold direction can be switched to allow
¹⁶ segmentation of the structure of interest in different imaging modalities, such as T1 and T2
¹⁷ weighted contrasts. The opacity of the mask and the brightness and contrast of the MRI
¹⁸ image can be adjusted via sliders. A 3D model of the thresholded mask can be computed to
¹⁹ inspect the result in an interactive 3D render. Finally, the thresholded mask, the space varying
²⁰ threshold and the list of control points can be saved for later use in scripted workflows, able to
²¹ reproduce the thresholded volume from the original data.
²²

²³ Statement of need

²⁴ Brain extraction and segmentation are required for most analyses of neuroimaging data.
²⁵ Obtaining appropriate masks can be particularly difficult in non-human brain imaging, as
²⁶ standard automatic tools struggle with the surrounding muscle tissue, skull, and strong
²⁷ luminosity gradients. A simple interactive threshold is intuitive and fast to apply, and can often
²⁸ provide a rather good initial guess. However, because of luminosity gradients, the threshold
²⁹ that works for one brain region is likely to fail in another.

³⁰ Thresholdmann complements the variety of existing brain segmentation tools, providing an
³¹ easy interface to manually control the segmentation on a local scale across different brain
³² imaging modalities and image contrast gradients. The masks produced by Thresholdmann
³³ can serve as a starting point for more detailed manual editing using tools such as BrainBox
³⁴ (<https://brainbox.pasteur.fr>) (Heuer et al., 2016) or ITK-SNAP (<http://www.itksnap.org>)
³⁵ (Yushkevich et al., 2006). This interactive approach is especially valuable for non-human brain
³⁶ imaging data, where automatic approaches often require extensive manual adjustment anyway
³⁷ (Messinger et al., 2020; Milham et al., 2020, 2022). We have used Thresholdmann successfully
³⁸ to create initial brain masks for a variety of vertebrate brains – including many non-human
³⁹ primate datasets (Heuer et al., 2019; Magielse et al., 2023) – as well as developmental data.
⁴⁰ Small Web tools, such as Thresholdmann or Reorient (<https://neuroanatomy.github.io/reorient>)
⁴¹ (Heuer & Toro, 2020), focused on solving a single problem, can become helpful additions to
⁴² the methodological toolbox of neuroimagers.

⁴³ Methods

⁴⁴ The spatially-varying threshold is computed from a number of control points. Each control
⁴⁵ point has a position x_i and a threshold value v_i that can be adjusted interactively. At each
⁴⁶ point x of the volume, the local threshold is computed as a weighted function of the control
⁴⁷ points. The weight associated to the i -th control point at position x is given by:

$$\text{48} \quad w_i(x) = \frac{1}{(x - x_i)^2 + \epsilon},$$

⁴⁹ where ϵ is a small number used to prevent a division by 0 at the exact position of control
⁵⁰ points. The value of the threshold at position x is obtained as:

$$\text{52} \quad v(x) = \frac{\sum_i^n v_i w_i(x)}{W(x)},$$

⁵³ where $W(x)$ is the sum of all weights, given by:

$$\text{55} \quad W(x) = \sum_i^n w_i(x).$$

⁵⁶ Additionally, we add a “background” threshold value which makes the action of the control
⁵⁷ points localised. The background value is independent of the distance and is given a small
⁵⁸ constant weight. In that manner, positions far from all control points get the background
⁵⁹ threshold value.

⁶⁰ Thresholdmann was coded in JavaScript and runs from a GitHub page. Code style was verified
⁶¹ using ESLint (<https://eslint.org>). Unit tests and end-to-end tests were implemented using
⁶² Mocha (<https://mochajs.org>) and Puppeteer (<https://pptr.dev>). Modifications in the code
⁶³ are continuously tested using CircleCI (<https://circleci.com>).

64 Figures

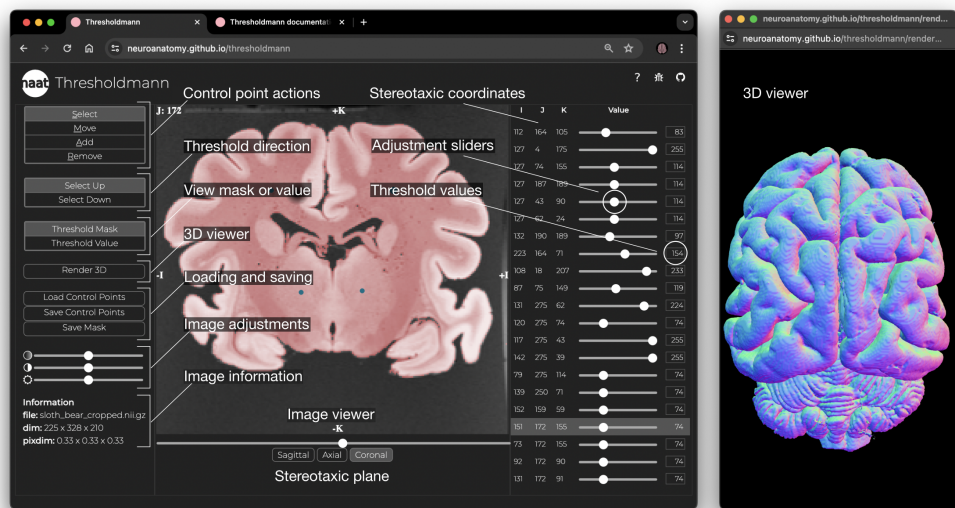


Figure 1: Interface and 3D viewer. The **left panel** allows to select different control point actions, set the thresholding direction, switch between the threshold mask or value view, open the 3D viewer, load or save the work, change the opacity of the mask, the brightness and contrast of the MRI, and information about the imaging data. The **central panel** is a stereotaxic viewer which allows the user to move through the slices using the slider at the bottom, to switch between the 3 stereotaxic planes, and to interactively set, move or remove control points. Users can view the threshold mask, or the corresponding threshold value space. The **right panel** shows for each control point the stereotaxic coordinates, an adjustment slider to change the local threshold, and the threshold value. The selected control point is highlighted in the panel and the viewer jumps to the corresponding slice. The **interactive 3D viewer** opens in a separate browser window.

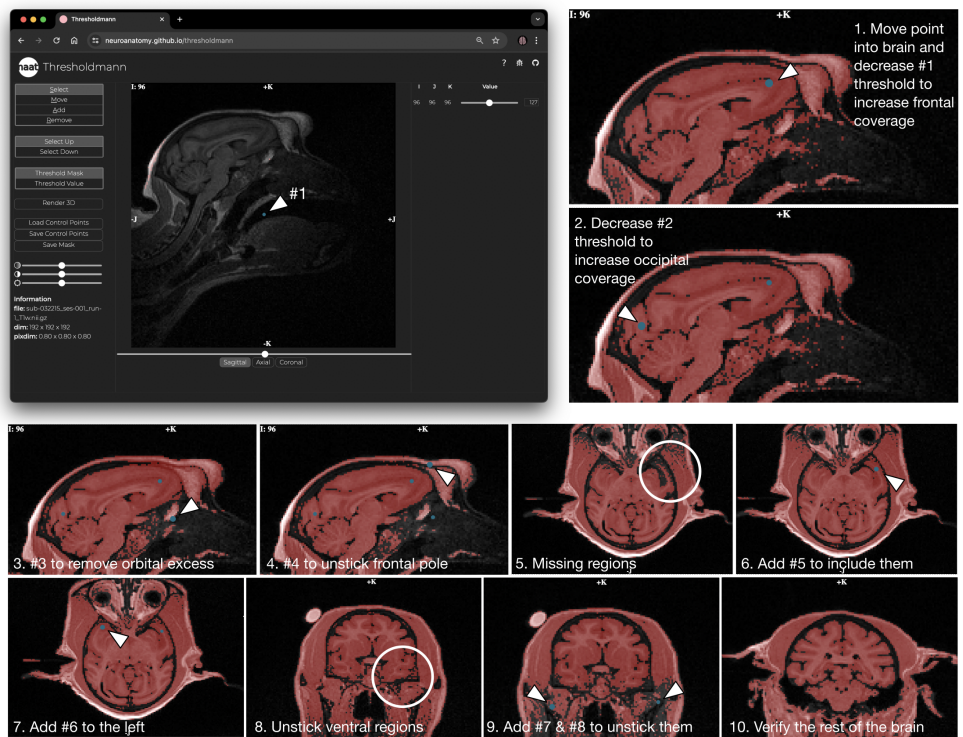


Figure 2: Usage example: Placing control points. Control points (blue dots) are added by clicking at the desired position in the viewer. This adds a slider to the right, which can be used to locally adapt the threshold. The figure describes the progressive addition of control points to create a mask of the brain for a macaque from Prime-DE site “amu” (Brochier et al., 2019; Milham et al., 2020).

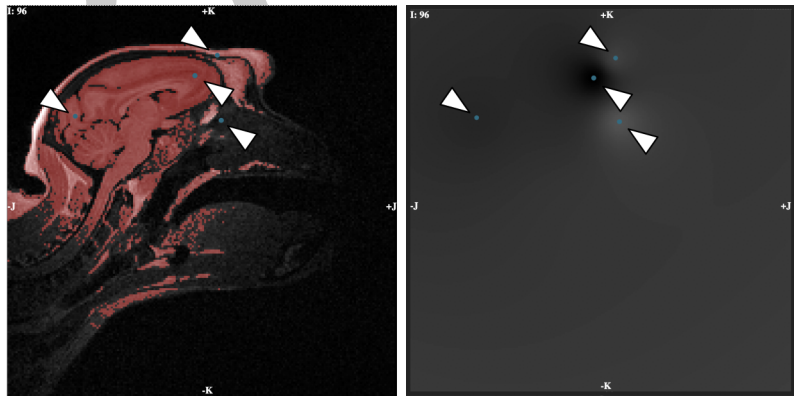


Figure 3: Usage example: Resulting mask and space-varying threshold. Threshold mask and corresponding threshold value. These volumes are updated in real time and can both be inspected interactively. The set of control points and the mask can be downloaded.

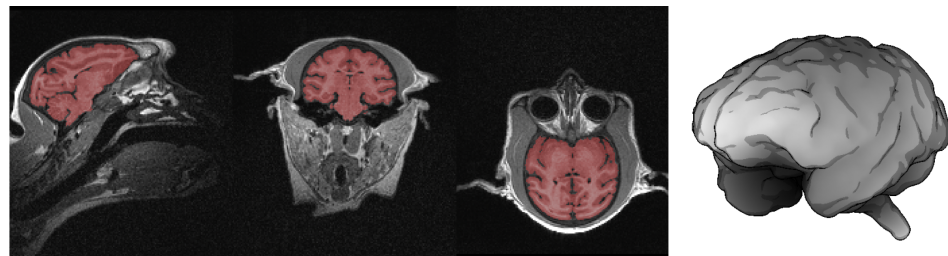


Figure 4: Usage example: Final mask. We downloaded the mask presented above based on the shown set of eight control points. The brain region was sufficiently disjoint from the rest of the head so that a mathematical morphology closing was enough to completely separate it. The figure shows stereotaxic planes and a surface reconstruction of the mask.

65 Acknowledgements

66 We thank Demian Wassermann for discussions about radial basis functions that inspired the
 67 first version of our tool. Funded by project DMOBE (ANR-21-CE45-0016) and the European
 68 Union's Horizon 2020 research and innovation programme under the Marie Skłodowska-Curie
 69 grant agreement No101033485 (KH Individual Fellowship).

70 References

- 71 Brochier, T., Belin, P., Chavanne, F., Velly, L., Bodin, C., Renaud, L., Martin, M., Boes, L.,
 72 Sein, J., Nazarian, B., & al., et. (2019). *Macaca mulatta structural and diffusion weighted*
 73 *MRI data*. Zenodo. <https://doi.org/10.5281/ZENODO.3402456>
- 74 Heuer, K., Ghosh, S., Robinson Sterling, A., & Toro, R. (2016). Open neuroimaging laboratory.
 75 *Research Ideas and Outcomes*, 2, e9113. <https://doi.org/10.3897/rio.2.e9113>
- 76 Heuer, K., Gulban, O. F., Bazin, P.-L., Osoianu, A., Valabregue, R., Santin, M., Herbin, M.,
 77 & Toro, R. (2019). Evolution of neocortical folding: A phylogenetic comparative analysis
 78 of MRI from 34 primate species. *Cortex*, 118, 275–291. <https://doi.org/10.1016/j.cortex.2019.04.011>
- 80 Heuer, K., & Toro, R. (2020). Reorient: A web tool for reorienting and cropping MRI data.
 81 *Journal of Open Source Software*, 5(55), 2670. <https://doi.org/10.21105/joss.02670>
- 82 Magielse, N., Toro, R., Steigauf, V., Abbaspour, M., Eickhoff, S. B., Heuer, K., & Valk, S. L.
 83 (2023). Phylogenetic comparative analysis of the cerebello-cerebral system in 34 species
 84 highlights primate-general expansion of cerebellar crura i-II. *Communications Biology*, 6,
 85 1188. <https://doi.org/10.1038/s42003-023-05553-z>
- 86 Messinger, A., Sirmpilatze, N., Heuer, K., Loh, K. K., Mars, R. B., Sein, J., Xu, T., Glen, D.,
 87 Jung, B., Seidlitz, J., & al., et. (2020). A collaborative resource platform for non-human
 88 primate neuroimaging. *NeuroImage*, 226, 117519. <https://doi.org/10.1016/j.neuroimage.2020.117519>
- 90 Milham, M., Petkov, C. I., Belin, P., Ben Hamed, S., Evrard, H., Fair, D., Fox, A., Froudast-
 91 Walsh, S., Hayashi, T., & al., et. (2022). Toward next-generation primate neuroscience: A
 92 collaboration-based strategic plan for integrative neuroimaging. *Neuron*, 110(1), 16–20.
 93 <https://doi.org/10.1016/j.neuron.2021.10.015>
- 94 Milham, M., Petkov, C. I., Margulies, D. S., Schroeder, C. E., Basso, M. A., Belin, P., Fair,
 95 D. A., Fox, A., Kastner, S., Mars, R. B., & al., et. (2020). Accelerating the evolution of
 96 nonhuman primate neuroimaging. *Neuron*, 105(4), 600–603. <https://doi.org/10.1016/j.neuron.2019.12.023>

- ⁹⁸ Yushkevich, P. A., Piven, J., Hazlett, H. C., Smith, R. G., Ho, S., Gee, J. C., & Gerig, G.
⁹⁹ (2006). User-guided 3D active contour segmentation of anatomical structures: Significantly
¹⁰⁰ improved efficiency and reliability. *NeuroImage*, 31(3), 1116–1128. <https://doi.org/10.1016/j.neuroimage.2006.01.015>

DRAFT